Determination and Simulation of the Mode I Fracture Toughness of Bamboo Scrimber

Guofang Wu,[a,b] Yingchun Gong,[a,b] Yong Zhong,[a,*] and Haiqing Ren [a,b]

Compact tension specimens were used to determine the mode I (opening crack) fracture toughness of bamboo scrimber, a bio-based product for engineering applications. The influence of thickness and grain mode were investigated, and the extended finite element method (XFEM) was used to simulate the fracture behavior of bamboo scrimber. The results showed that all of the specimens failed in a brittle way. There were no significant differences in fracture toughness among specimens with different thicknesses; however, the grain mode did have a significant effect. The average fracture toughness K_{IC} for T-L and R-L grain modes of bamboo scrimber were 54.32 MPa·mm$^{1/2}$ and 47.91 MPa·mm$^{1/2}$, respectively, where the letter "L" represents the longitudinal direction, "R" represents the stack direction, and "T" represents the flattened tangential direction. Based on the results, compact tension specimens with a thickness of 10 mm are recommended to measure the mode I fracture toughness of bamboo scrimber. Furthermore, XFEM was confirmed as a useful tool to investigate the fracture behavior of bamboo scrimber.

Keywords: Bamboo scrimber; Compact tension specimen; Fracture toughness; XFEM

*Contact information: a: Research Institute of Forestry New Technology, Chinese Academy of Forestry, Beijing, 100090, China; b: Research Institute of Wood Industry, Chinese Academy of Forestry, Beijing, 100090, China; *Corresponding author: zhongy@caf.ac.cn*

INTRODUCTION

Because of the growing consciousness of sustainable development, bio-based materials are becoming increasingly popular in building industries around the world. Biomaterials such as wood and bamboo play a major role in sequestering carbon, and they require less energy than most other building materials in the life cycle of a building (Amada *et al*. 1997; Kuehl *et al*. 2013). Bamboo can be harvested in 3 to 5 years, which is much shorter than trees, yet its strength-to-weight ratio is similar to or greater than wood (Nogata and Takahashi 1995; Albermani *et al*. 2007). As bamboo is extensively grown in sub-tropical and tropical areas with rapidly developing economies, it is one of the most promising alternative building materials to concrete and steel.

Plants such as bamboo and trees are not designed for use as building materials. The tubular stem of bamboo is meant to support its own weight and heavy loads on the branches created by snow, wind, *etc*. Raw bamboo is not a standardized product due to variability in its size and mechanical properties, along with other defects. There have been efforts to turn bamboo into construction materials suitable for the modern building industry (Xiao *et al*. 2013; Correal *et al*. 2014; Li *et al*. 2015).

Bamboo scrimber, a compressed or laminated product manufactured with bamboo and thermosetting resin, is an innovative bamboo-based product that is very popular in China. The latest manufacturing technology, improved by Yu and Yu (2013), is shown in Fig. 1. First, the bamboo culm is split into halves, and the inner nodes are removed. The

semicircular culms are crushed and flattened into oriented bamboo fiber mats (OBFM) with a netlike structure. After oven-drying, these mats are immersed into resin and dried to a specific moisture content. The OBFM are stacked into a cuboid mold layer-by-layer and hot-pressed into the bamboo scrimber. Bamboo scrimber has great potential as an engineering and building material due to its high manufacturing efficiency, material utilization rate, and good mechanical properties (Yu *et al*. 2014). For engineering applications, the mechanical properties and design strength of bamboo scrimber have been investigated (Yu *et al*. 2006; Zhu *et al*. 2011; Zhong *et al*. 2014).

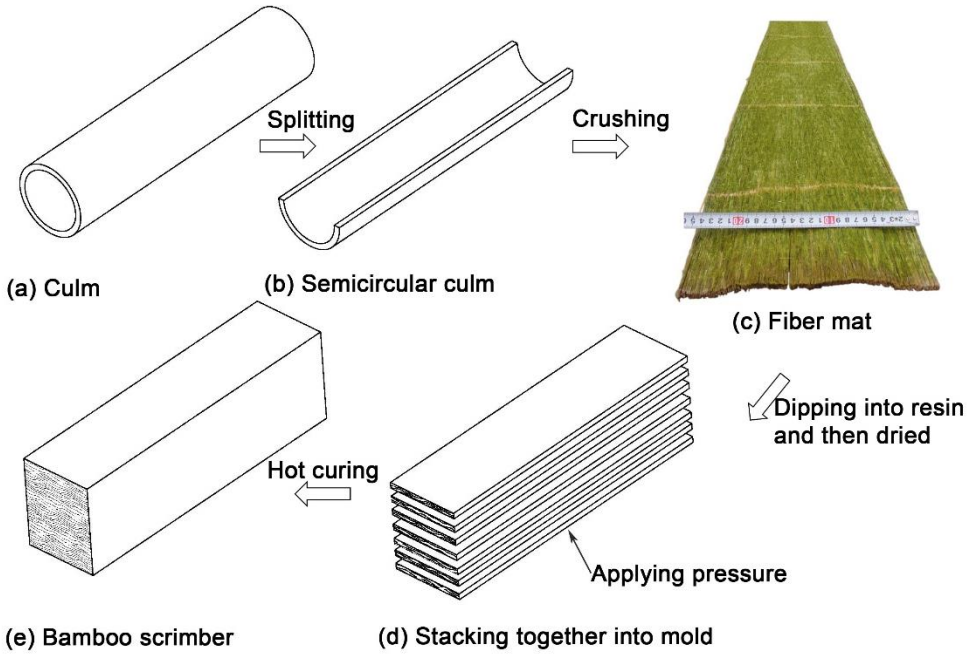

Fig. 1. The manufacturing process of bamboo scrimber

Micro-cracks are inevitably introduced into the bamboo scrimber members and may affect the structural performance. The bamboo culms are passed through a fluffing machine, and many linear cracks form in the culms. Cracks may also appear at the bonding interface between two layers of bamboo mats because the waxy layer in the outer skin of bamboo damages the glue line. These micro-cracks were extensively distributed in bamboo scrimber, and may induce the failure of the bamboo scrimber under enteral force or action (Liu 2016). Fracture due to the micro-cracks were observed not only in bamboo scrimber (Sharma *et al*. 2015), but also in other engineered bamboo products like bamboo bundle laminated veneer lumber (Chen *et al*. 2014).

The authors developed one type of reinforced bamboo scrimber composite (RBSC) beam and investigated its bending properties by experiment. When the beam was loaded to failure, cracking across the neutral plane of the beam occurred in some specimens, and the bearing capacity of these beams was much lower than those of beams that failed due to tension of the bamboo fiber (Zhong *et al*. 2017). Thus, the fracture mechanics may be used to predict the failure load of the bamboo scrimber members.

Fracture toughness is the ability of a material containing cracks to resist fracture. There are three ways of applying a force that enable the crack to propagate: mode I, the opening crack; mode II, the sliding crack; and mode III, the tearing crack. For biomaterials

such as wood and bamboo, the tension strength in its perpendicular-to-grain direction is significantly lower than that in its parallel-to-grain direction, so the opening mode is usually the most critical. The fracture properties of raw bamboo of some species have been investigated (Shao *et al*. 2009; Wang *et al*. 2014; Xu *et al*. 2014), and the fracture characteristics of a kind of bamboo fiber-based polyester were investigated by Wong *et al*. (2010), while the authors have investigated the mode II fracture toughness (Wu *et al*. 2018). However, the mode I fracture toughness of bamboo scrimber has not yet been reported.

The objectives of this study were to determine the feasibility of using compact tension specimens to measure the mode I fracture toughness of bamboo scrimber, to evaluate the effects of thickness and grain orientation on the fracture toughness, and to verify whether the fracture mechanics can be used to describe the cracking behavior of bamboo scrimber by the extended finite element method (XFEM).

EXPERIMENTAL

Materials

The specimen was cut from a bamboo scrimber beam whose bending property was evaluated by Zhong *et al*. (2017). The dimensions of the bamboo scrimber beam were 3600 mm × 150 mm × 150 mm. The raw bamboo was 3-year-old to 4-year-old moso bamboo (*Phyllostachys pubescens*) collected from the Anhui province of China. And the resin used to produce the bamboo scrimber was a commercially available low molecular weight phenol formaldehyde resin (PF16L510) supplied by Beijing Dynea Chemical Industry Co. Ltd. The resin accounted for about 12.5% of the total weight of the bamboo scrimber products. The density of the bamboo scrimber was 1.03 g/cm^3 with a standard deviation of 0.06 g/cm^3. The tension strength, compression strength, and shear strength parallel to the grain of the bamboo scrimber were 139.3 MPa, 87.93 MPa, and 20.77 MPa, respectively, and the corresponding standard deviation were 17.2 MPa, 9.74 MPa, and 3.26MPa, respectively (Zhong *et al*. 2017).

As a new product, there is still no standard procedure to determine the fracture toughness. However, compact tension specimens are suitable to test the mode I fracture toughness of wood (Shao *et al*. 2002) and raw bamboo fiber-based polyester (Wong *et al*. 2010). Therefore, the compact tension specimens were chosen to investigate the mode I fracture toughness of the bamboo scrimber.

Figure 2 shows the dimensions of the compact tension specimen. The outline of the specimen was 62.5 mm × 60 mm. One 34.5-mm-long gap was cut along the longitudinal direction, with a slit of approximately 3 mm inserted at the end of the gap using a 0.28-mm-thick razor blade. One hole was drilled in each fork. Specimens with thicknesses of 10 mm, 20mm, and 30 mm were designed to investigate the effect of the thickness on the fracture toughness. Two types of specimens with different grain modes were cut from the bamboo scrimber beam, *i.e*., the T-L and R-L specimens, named using a two-letter code. The first letter designates the direction normal to the crack plane, while the second letter denotes the expected direction of crack propagation. The letter "L" represents the longitudinal direction. Because the culm was flattened, and the bamboo mats were stacked layer-by-layer, "R" represents the stack direction, and "T" represents the flattened tangential direction. As shown in Fig. 3, the grain directions can be clearly observed on the end surface of the specimen. There were 9 replicates for each thickness and grain mode, and a total of 54 specimens were manufactured.

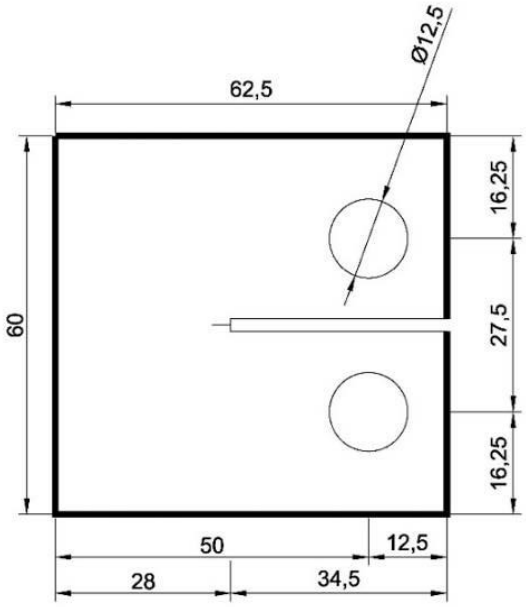

Fig. 2. Dimensions (in mm) of the compact tension specimen

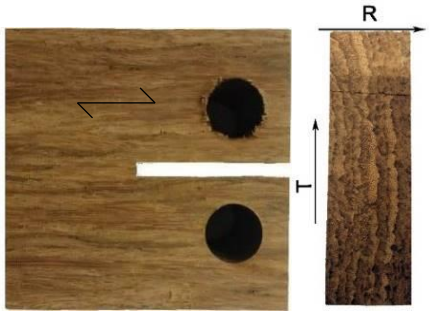

Fig.3. Photo of a specimen and the grain directions

Fig. 4. Test setup

Test Procedure

As shown in Fig. 4, the load was applied to the specimen *via* the U-shaped clamps. A double-cantilever clip-in displacement gauge was mounted to the crack to trace the opening of the crack. A crosshead speed of 0.5 mm/min was chosen according to the work of Liu (2009). The tests were performed at room temperature (approximately 20 °C).

XFEM Modeling

The cracking behavior can be studied using XFEM, which allows the presence of discontinuities in an element by enriching degrees of freedom with special displacement functions. In this study, four-node plane strain elements (CPE4R) were used to model the specimen in Abaqus 6.14 (Dassault Systèmes Simulia Corp., Providence, RI, USA). A 3-mm initial crack was inserted into the same position with the specimen, and the whole specimen was assigned as the crack propagation region. The mesh in the anticipated crack propagation region was refined. A reference point at the center of each hole was coupled to the nodes around the hole, and then the translational movements of one reference point were restrained, while a vertical movement was assigned to the other reference point. The maximum-principal-stress criterion used to model the crack initiation can be expressed by Eq. 1,

$$f = \frac{\langle \sigma_{\mathrm{n}} \rangle}{\sigma_{\mathrm{max}}^{0}} \quad (1)$$

where $\langle \sigma_{\mathrm{n}} \rangle$ is the actual principal stress, and $\sigma_{\mathrm{max}}^{0}$ is the maximum principal stress. Initiation occurs when the maximum principal stress reached (f = 1). Displacement-based damage evolution was chosen. The finite element model is shown in Fig. 5.

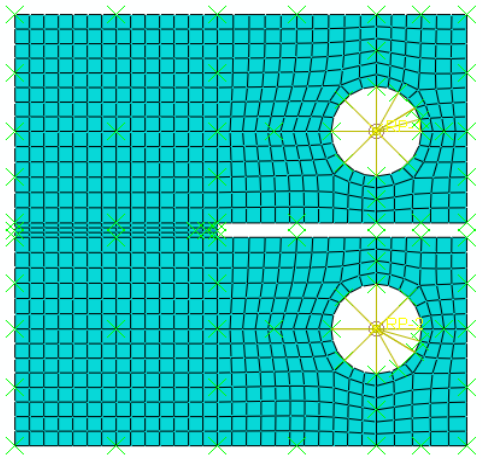

Fig. 5. The extended finite element model

RESULTS AND DISCUSSION

Failure Mode

As shown in Fig. 6, failure occurred at the crack tip instantaneously, and the crack propagated unstably. In some specimens, fiber bridging was observed, as shown in Fig.

6(b). This was similar to wood (Wu *et al*. 2012); however, it was very easy to separate the two parts artificially.

The failure surface of the specimens in the T-L group was generally coarser than that of the specimens in the R-L group, as illustrated in Fig. 7. This result might be because the crack can propagate in a zigzag fashion due to micro-cracks at the bonding interface which was perpendicular to the initial cracking surface in the T-L group, while the crack usually propagated within the same layer of OBFM in the R-L group.

Fig. 6. Fracture of the specimen: (a) crack of the specimen and (b) fiber bridging

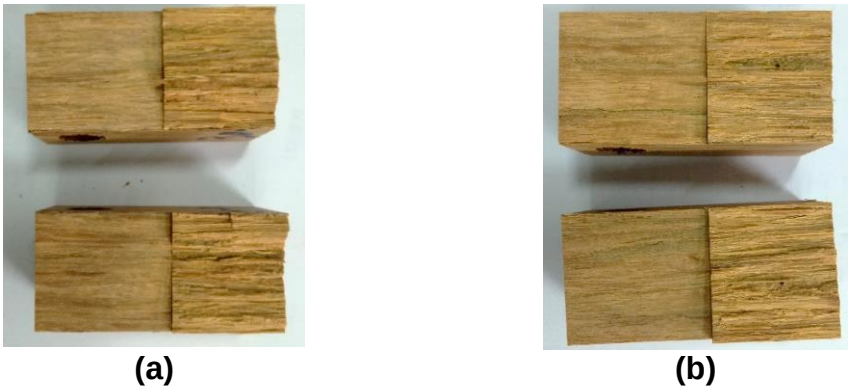

Fig. 7. Failure surfaces of specimens: (a) T-L and (b) R-L

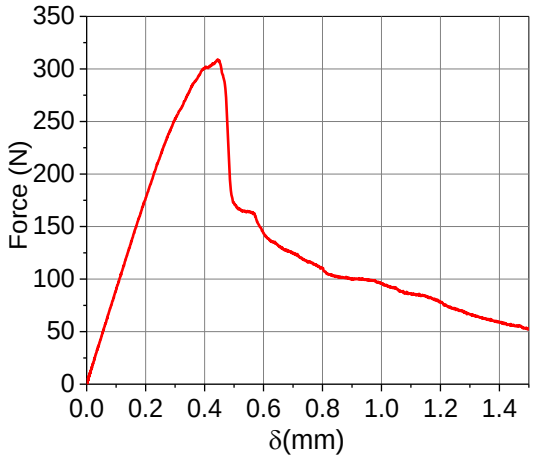

Fig. 8. Typical load-displacement curve

Figure 8 shows a typical load-crack opening displacement curve of the specimen. The relationship between load and displacement was generally linear before the peak load, after which the load decreased sharply. Therefore, the peak load of each specimen was taken as the critical load that initiated the crack.

Test Results

The compact tension specimen's critical stress intensity factor (K_{IC}) can be obtained by the equation recommended by ASTM E399-17 (2017) as,

$$K_{IC} = \left(\frac{F_Q}{BW^{1/2}} \right) f(a/W) \tag{2}$$

where F_Q is the critical load, B is the thickness of the specimen, W is the height of the specimen, a is the length of the initial crack, and $f(a/W)$ is a geometry factor, which for the compact tension specimen can be expressed as:

$$f(r) = \frac{2+r}{(1-r)^{1.5}} (0.866 + 4.64r - 13.32r^2 + 14.72r^3 - 5.06r^4) \tag{3}$$

Schachner *et al*. (2000) verified that Eq. 2 could be used to calculate the stress intensity factor of parallel-to-the-grain mode I cracking in wood *via* the finite element method. In this study, the same equation was adopted for bamboo scrimber. The fracture toughness (K_{IC}) for each specimen is listed in Table 1. The average, standard deviation, and coefficient of variation for each group and each grain direction are also presented.

Table 1. K_{IC} of the Bamboo Scrimber

	K_{IC} (MPa·mm$^{1/2}$)					
Grain Mode	T-L			R-L		
Thickness	10 mm	20 mm	30 mm	10 mm	20 mm	30 mm
1	69.32	63.40	55.78	49.90	54.42	40.01
2	55.16	53.53	59.81	59.23	47.81	57.47
3	52.59	64.07	60.51	35.30	51.30	50.37
4	50.33	46.01	48.40	53.99	39.29	61.32
5	43.18	53.97	51.46	37.73	53.42	41.59
6	56.81	52.38	53.01	48.83	47.99	46.48
7	49.20	60.22	62.32	50.27	40.84	50.75
8	44.64	52.12	52.37	43.63	46.72	49.23
9	-	-	47.30	42.13	45.74	-
Average	54.32			47.91		
	52.65	55.71	54.55	46.78	47.50	49.65
Standard Deviation	6.51			6.62		
	8.22	6.27	5.39	7.73	5.16	7.24
Coefficient of Variation	0.12			0.14		
	0.16	0.11	0.10	0.17	0.11	0.15

One-way analysis of variance (ANOVA) was conducted for each test group and between the two grain modes. Within the same grain mode, there were no significant differences among the thicknesses (p=0.66 and p=0.67 for different thicknesses in T-L

grain mode and R-L grain mode, respectively); however, there was a significant difference between the two grain modes(p=0.0007). Therefore, 10 mm was thick enough for the stress to be distributed uniformly throughout the thickness of the specimen.

Table 1 shows that the average K_{IC} values of bamboo scrimber for the T-L and R-L grain modes were 54.3 MPa·mm$^{1/2}$ and 47.9 MPa·m$^{1/2}$, respectively. Thus, the fracture toughness of the T-L grain mode was 13.4% greater than in the R-L grain mode. One possible reason for this phenomenon was that the bonding strength at the interface was weakened by the waxy coat in the outer layer of the bamboo. Furthermore, the fracture toughness of the T-L group was more uniform than in the R-L group. The results were similar to the results for fiber-reinforced polyester composites, which was around 50 MPa·mm$^{1/2}$ (Wong *et al*. 2010).

The strain energy release rate is another important index to represent the fracture toughness. For orthotropic materials, the critical strain energy release rate (G_{IC}) can be calculated from K_{IC} as,

$$G_{IC} = \frac{K_{IC}^2}{E^*} \tag{4}$$

$$E^* = \frac{\sqrt{2E_L E_{T(R)}}}{\sqrt{\sqrt{E_L / E_{T(R)}} + \sqrt{E_L / \left(2G_{LT(R)}\right)}}} \tag{5}$$

where E_L, E_T, and E_R represent the modulus of elasticity in the parallel, tangential, and radial directions, respectively, and G_{LT} and G_{LR} represent the shear modulus in the LT and LR planes. As calculated, the G_{IC} values in the T-L plane and R-L plane were 1.18 N/mm and 0.55 N/mm, respectively. In contrast, the fracture toughness of raw bamboo was approximately 0.36 N/mm (Shao *et al*. 2002). Thus, the fracture toughness of the bamboo scrimber was greater than that of raw bamboo, *i.e*., the fracture toughness of raw bamboo was improved by the manufacturing technology. This result was similar to the trend of mode II fracture toughness (Wu *et al*. 2018) and other mechanical properties such as the compression strength (Zhong *et al*. 2017).

Simulated Results

The simulation problem was solved using the Abaqus Standard solver. Figure 9 shows the crack and the perpendicular stress contour of the specimen. Because it was a 2-dimensional model, there was no thickness information in the model. Therefore, the unit thickness was used to calculate the fracture toughness.

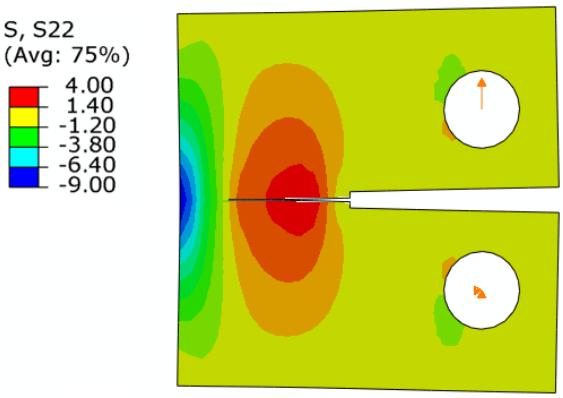

Fig. 9. Stress contour of the specimen

The predicted fracture toughness values for the T-L and R-L grain modes were 43.85 MPa·mm$^{1/2}$ and 39.78 MPa·mm$^{1/2}$, which were 19.3% and 17.0% lower than the test results, respectively. The error mainly resulted from the varied mechanical properties of bamboo scrimber and the assumptions made in the calculation, such as the orthotropic material assumption. And it may also due to of mechanical properties differences because all of the fracture specimens were cut from one bamboo scrimber beam; however, the specimens for mechanical properties were cut from other beams in the same batch of products. The error of the prediction was judged to be acceptable. It provides an optional way to investigate the fracture toughness of the bamboo scrimber, and the method can be used to investigate the structural performance of bamboo scrimber members.

CONCLUSIONS

1. The average fracture toughness (K_{IC}) values for the T-L and R-L grain modes of the bamboo scrimber were 54.3 MPa·mm$^{1/2}$ and 47.9 MPa·mm$^{1/2}$, respectively. The difference mainly resulted from the specific structure of the products.
2. There was no significant difference among the fracture toughness (K_{IC}) values of specimens ranging from 10 mm to 30 mm in thickness. Therefore, 10-mm-thick compact specimens can be used to measure the mode I fracture toughness of the bamboo scrimber.
3. The failure of the bamboo scrimber specimens was instantaneous, which means that the plastic strain in the crack tip before failure was small. Thus, the linear elastic fracture mechanics was applicable to the mode I fracture of the bamboo scrimber.
4. The extended finite element method (XFEM) could be used to simulate the fracture of the bamboo scrimber, and the error of prediction was within an acceptable range.

ACKNOWLEDGMENTS

The authors are grateful for the financial support from the National Key R&D Program of China (Grant No. 2017YFC0703501) and the Fundamental Research Funds of Research Institute of Forestry New Technology, Chinese Academy of Forestry (Grant No. CAFYBB2017SY036).

REFERENCES CITED

Albermani, F., Goh, G. Y., and Chan., S. L. (2007). "Lightweight bamboo double layer grid system," *Engineering Structures* 29(7), 1499-1506. DOI: 10.1016/j.engstruct.2006.09.003

Amada, S., Ichikawa, Y., Munekata, T., Nagase, Y., and Shimizu, H. (1997). "Fiber texture and mechanical graded structure of bamboo," *Composites Part B: Engineering* 28(1-2), 13-20. DOI: 10.1016/S1359-8368(96)00020-0

ASTM E399-17 (2017). "Standard test method for linear-elastic plane-strain fracture toughness KIc of metallic materials," ASTM International, West Conshohocken, PA,

USA.

Chen, F., Deng, J., Cheng, H., Li, H., Jiang, Z., Wang, G., Zhao, Q., and Shi, S.-q. (2014). "Impact properties of bamboo bundle laminated veneer lumber by preprocessing densification technology," *Journal of Wood Science* 60(6), 421-427. DOI: 10.1007/s10086-014-1424-0

Correal, J. F., Echeverry, J. S., Ramírez, F., and Yamín, L. E. (2014). "Experimental evaluation of physical and mechanical properties of glued laminated *Guadua angustifolia* Kunth," *Construction and Building Materials* 73, 105-112. DOI: 10.1016/j.conbuildmat.2014.09.056

Kuehl, Y., Li, Y., and Henley, G. (2013). "Impacts of selective harvest on the carbon sequestration potential in Moso bamboo (*Phyllostachys pubescens*) plantations," *Forests, Trees and Livelihoods* 22(1), 1-18. DOI: 10.1080/14728028.2013.773652

Li, H.-t., Su, J.-w., Zhang, Q.-s., Deeks, A. J., and Hui, D. (2015). "Mechanical performance of laminated bamboo column under axial compression," *Composites Part B: Engineering* 79, 374-382. DOI: 10.1016/j.compositesb.2015.04.027

Liu, X. (2016). *Study on the Damage and Fracture of Reconstituted Bamboo*, Master's Thesis, Chongqing Jiaotong University, Chongqing, China, 2016.

Liu, Y. (2009). *Perpendicular to Grain Fracture of Curved Glulam Beams - Experiment and Numerical Modelling*, Master's Thesis, Harbin Institute of Technology, Harbin, China.

Nogata, F., and Takahashi, H. (1995). "Intelligent functionally graded material: Bamboo," *Composites Engineering* 5(7), 743-751. DOI: 10.1016/0961-9526(95)00037-N

Schachner, H., Reiterer, A., and Stanzl-Tschegg, S. E. (2000). "Orthotropic fracture toughness of wood," *Journal of Materials Science Letters* 19(20), 1783-1785. DOI: 10.1023/A:1006703718032

Shao, Z.-P., Fang, C.-H., and Tian, G.-L. (2009). "Mode I interlaminar fracture property of moso bamboo (*Phyllostachys pubescens*)," *Wood Science and Technology* 43(5-6), 527-536. DOI: 10.1007/s00226-009-0265-2

Shao, Z., Jiang, Z., and Ren, H. (2002). "The particularity of application of principles of linear-elastic fracture mechanics to wood and fracture parallel to grain," *Scientia Silvae Sinicae* 38(6), 110-115. DOI: 10.11707/j.1001-7488.20020619

Sharma, B., Gatóo, Ana, Bock, M., and Ramage, M. (2015). "Engineered bamboo for structural applications," *Construction and Building Materials* 81, 66-73. DOI: 10.1016/j.conbuildmat.2015.01.077

Wang, F., Shao, Z., Wu, Y., and Wu, D. (2014). "The toughness contribution of bamboo node to the mode I interlaminar fracture toughness of bamboo," *Wood Science and Technology* 48(6), 1257-1268. DOI: 10.1007/s00226-013-0591-2

Wong, K. J., Zahi, S., Low, K. O., and Lim, C. C. (2010). "Fracture characterisation of short bamboo fibre reinforced polyester composites," *Materials & Design* 31(9), 4147-4154. DOI: 10.1016/j.matdes.2010.04.029

Wu, G., Zhong, Y., Gong, Y., and Ren, H. (2018). "Mode II fracture toughness of bamboo scrimber with compact shear specimen," *BioResources* 13(1), 477-486. DOI: 10.15376/biores.13.1.477-486

Wu, Y., Shao, Z., and Wang, F. (2012). "Study on wood fracture parallel to the grains based on fractal geometry," *International Journal of Fracture* 176(2), 163-169. DOI: 10.1007/s10704-012-9732-0

Xiao, Y., Yang, R. Z., and Shan, B. (2013). "Production, environmental impact and

mechanical properties of glubam," *Construction and Building Materials* 44(3), 765-773. DOI: 10.1016/j.conbuildmat.2013.03.087

Xu, M., Wu, X., Liu, H., Sun, Z., Song, G., Zhang, X., and Zhao, S. (2014). "Mode I fracture toughness of tangential moso bamboo," *BioResources* 9(2), 2026-2032. DOI: 10.15376/biores.9.2.2026-2032

Yu, W.-j., Yu, Y.-l., Zhou, Y., and Ren, D.-h. (2006). "Studies on factors influencing properties of reconstituted engineering timber made from small-sized bamboo," *China Forest Products Industry* 33(6), 24-28. DOI: 10.3969/j.issn.1001-5299.2006.06.006

Yu, Y., and Yu, W. (2013). "Manufacturing technology of bamboo-based fiber composites with high-performance," *World Bamboo and Rattan* 11(3), 6-10.

Yu, Y., Huang, X., and Yu, W. (2014). "A novel process to improve yield and mechanical performance of bamboo fiber reinforced composite *via* mechanical treatments," *Composites Part B: Engineering* 56, 48-53. DOI: 10.1016/j.compositesb.2013.08.007

Zhong, Y., Jiang, Z., Shangguan, W.-W., and Ren, H.-Q. (2014). "Design value of the compressive strength for bamboo fiber-reinforced composite based on a reliability analysis," *BioResources* 9(4), 7737-7748. DOI: 10.15376/biores.9.4.7737-7748

Zhong, Y., Wu, G., Ren, H., and Jiang, Z. (2017). "Bending properties evaluation of newly designed reinforced bamboo scrimber composite beams," *Construction and Building Materials* 143, 61-70. DOI: 10.1016/j.conbuildmat.2017.03.052

Zhu, R.-x., Zhou, Y., Ren, D.-h., Yu, Y.-l., and Yu, W.-j. (2011). "Effect of manufacturing methods on bamboo-fiber based composite performance," *China Wood Industry* 25(3), 1-3. DOI: 10.3969/j.issn.1001-8654.2011.03.001

Article submitted: March 7, 2019; Peer review completed: May 25, 2019; Revised version received: June 28, 2019; Accepted: July 1, 2019; Published: July 8, 2019.
DOI: 10.15376/biores.14.3.6811-6821